



## Sensitivity of test procedures for vibration-based damage detection on a multi-girder bridge superstructure

Yufeng Wang<sup>1</sup>, Leon D. Wegner<sup>2</sup>, and Bruce F. Sparling<sup>2</sup>

<sup>1</sup> March Consulting Associates Inc., Saskatoon, Canada

<sup>2</sup> Department of Civil and Geological Engineering, University of Saskatchewan, Saskatoon, Canada

**ABSTRACT:** Vibration-based damage detection (VBDD) techniques have been proposed as a potential form of structural health monitoring with which an entire structure can be evaluated simultaneously using relatively few sensors. Since these methods rely on the identification of small changes in dynamic properties (notably natural frequencies and mode shapes) to infer the existence and the location of damage, reliable estimates of these properties are essential for the successful implementation of VBDD schemes. Depending on the specific test procedures followed, different levels of experimental uncertainty are experienced, leading to variations in the sensitivity to changes in the structural condition. An experimental study was therefore carried out to identify test procedures that would result in the greatest sensitivity to damage. Data for the study were generated using a one-third scale slab-on-girder composite bridge superstructure model. A damage detection indicator was developed based on mode shapes that had been normalized to enclose an area of unity. The resulting area under the plot of differences between two independently measured mode shapes was then used as the damage indicator. A database of pairs of independently measured mode shapes, in which each mode shape in the pair was obtained from the structure in an identical condition, was used to ascertain the variability of the area of mode shape change indicator when different test procedures were followed. This allowed the definition of a threshold value for each set of test procedures, corresponding to the 95<sup>th</sup> percentile upper exclusion limit of the statistical distribution of the damage indicator. A total of 21 different test protocols were investigated, which included two different excitation methods, three different instrumentation schemes, and five different vibration modes. The area of mode shape change calculated for three separate damage cases using different test protocols was compared to the threshold values. Results showed that the lowest threshold levels were achieved using resonant harmonic excitation of the fundamental mode, regardless of whether acceleration or strain measurements were used. These protocols permitted all three damage cases to be successfully detected, while the use of white noise random excitation only resulted in successful identification of damage when acceleration measurements were used.

### 1 INTRODUCTION

Due to the aging of materials, environment-related corrosion, overuse, overloading, and an absence of sufficient maintenance, the existing inventory of bridges world-wide continues to experience structural degradation (Shrive 2005). To manage the resulting requirements for maintenance, rehabilitation or reconstruction in a rational manner, there is an increasing need for effective structural health monitoring (SHM) of bridges.

Vibration-based damage detection (VBDD) techniques have been proposed as a potential form of SHM with which the entire structure can be evaluated simultaneously using relatively few sensors. The basis for this approach is that damage to a structure will modify its global dynamic characteristics (notably natural frequencies and mode shapes). In theory, since these dynamic characteristics are readily quantifiable and can be related directly to specific physical properties of the structure, any measurable changes over time may be used to detect, locate and possibly quantify damage at an early stage before visible signs of distress are apparent.

Since these methods rely on the identification of small changes in dynamic properties to infer the nature of the damage, though, reliable estimates of these properties are essential for a successful implementation of VBDD schemes (Wegner et al. 2004). However, all experimental procedures result in a certain degree of uncertainty. The current study therefore focused on identifying specific test procedures or protocols that would produce the lowest levels of uncertainty, and therefore produce the greatest likelihood of detecting damage using VBDD methods. These protocols were then tested experimentally using three discrete damage states.

## 2 EXPERIMENTAL PROGRAM

### 2.1 Description of bridge model

The structure used for this investigation was a one-third scale model of a slab-on-girder composite bridge superstructure featuring four steel girders supporting a steel-free concrete deck (Fig. 1). The W410X39 girders had a simple span of 8 m and were spaced at 900 mm on centre, while the deck had a total length of 8.16 m (edge to edge), a 3.6 m width, and a thickness of 75 mm at midspan and 100 mm over girders. To provide the necessary lateral restraint for the steel-free deck, the top flanges of the girders were connected by steel straps spaced at 800 mm, located as shown in Fig. 2. Diaphragms composed of cross-braced structural angles were placed at 12 locations to enhance load sharing between girders and provide lateral stability (denoted as D-Xx.xYy.y on Fig. 2).

To facilitate the subsequent introduction of well-defined and controlled damage states, a number of bolted member splices and end connections were incorporated into the model. First, a splice joint was introduced at the mid-span of Girder 4 (see the inset in Fig. 1) at the location shown in Fig. 2 (denoted as SP-X4.0Y2.7). Splice joints were also included at five locations on the steel straps (denoted as ST-Xx.xYy.y on Fig. 2). Finally, all diaphragm angle members featured bolted end connections so that any one or any combination of these members could be easily disconnected.



Figure 1. Slab on girder bridge superstructure built at 1/3<sup>rd</sup> scale (with inset showing the girder splice).

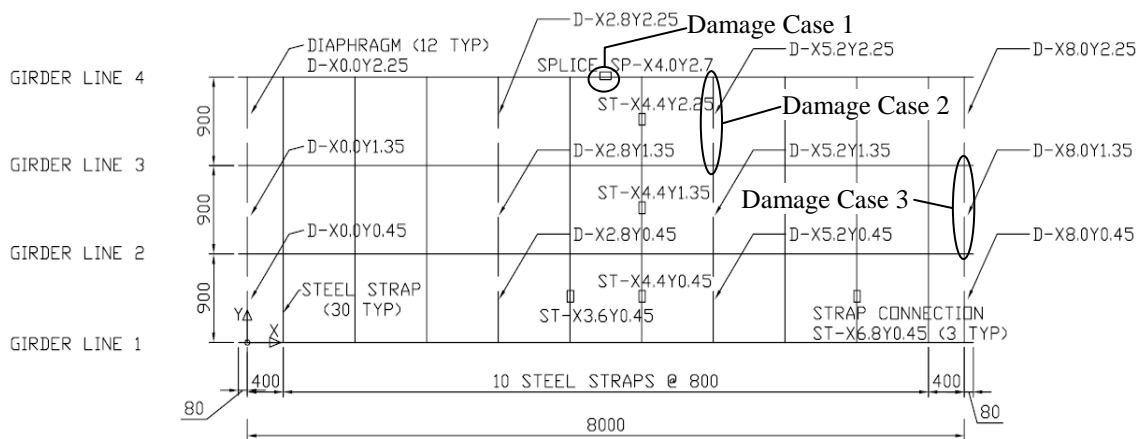


Figure 2. Plan view of the structural steel superstructure of the model showing splice and diaphragm locations (dimensions in mm).

## 2.2 Measurement of dynamic properties

Measurement of the dynamic properties of the bridge superstructure model was carried out in two stages. Initially, extensive dynamic tests were conducted to investigate the variability of the measurements when various specific test protocols were followed. These data were used to establish the *resolution* of each test protocol, defined as the threshold value of the damage indicator above which a change could be considered statistically significant, given the level of uncertainty. Subsequently, 17 damage states of relatively low severity were introduced to study the performance of selected VBDD indicators.

Forced dynamic excitation was provided by means of a hydraulic shaker, consisting of a hydraulic cylinder mounted vertically in the centre of a steel frame, with a steel plate of a selected mass supported at the bottom end of the cylinder. A feedback-controlled signal for the shaker plate motion was generated using LabView™ 8.0 software and monitored using a linear displacement transducer (LDT). The shaker was securely attached to the surface of the bridge deck at locations chosen to excite the vibration modes of interest.

Instrumentation used to measure the dynamic response included a closely-spaced grid of accelerometers (Kinemetrics EpiSensor FBA ES-U) mounted on the surface of the deck along the girder lines, as well as 6 mm long electrical-resistance foil strain gauges bonded to the girder webs in vertically aligned sets of three gauges to facilitate the determination of girder curvatures. The plan locations of the accelerometers and groups of strain gauges are indicated in Fig. 3. In total, 28 accelerometer locations and 57 strain gauges (19 sets of 3 gauges each) were monitored. Due to data acquisition limitations, though, five separate setups for the accelerometers were used, each featuring seven accelerometers; to permit normalization of all readings to a common basis, stationary reference sensors were included in all setups. In subsequent discussions, the three strain gauges at each instrumented girder web location are designated as the bottom, middle, and top strain gauges, which were located, respectively, 313, 208, and 103 mm below the neutral axis.

Data were acquired using a 12-bit data acquisition system consisting of a NI PCI-6024E data acquisition card and a model SCXI-1001 data acquisition chassis from National Instruments™, along with several modules used to acquire and modulate sensor signals. The data acquisition system was controlled by LabView™ software installed on a personal computer.

To identify the natural frequencies of the system for each condition tested, white noise random signals were initially used to excite the bridge deck, while data were acquired at 1000 samples

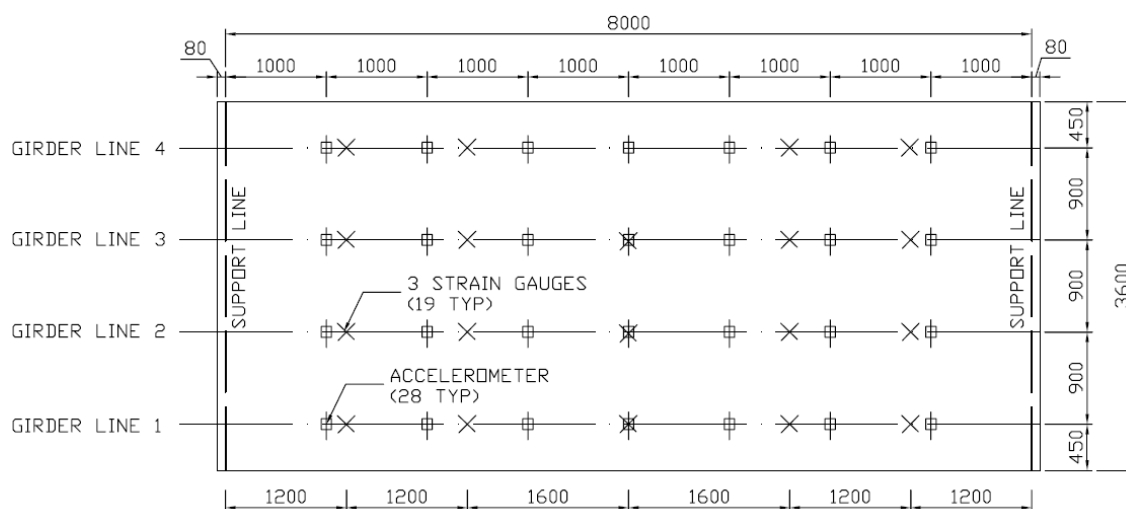


Figure 3. Plan view of bridge deck, showing the locations of accelerometers and strain gauge clusters (dimensions in mm).

per second over a period of 80 seconds. In this manner, the natural frequencies for the first five vibration modes of the undamaged model were found to be 12.70, 13.89, 34.56, 35.89, and 38.83 Hz. After the natural frequencies had been identified, further testing using harmonic excitation applied at each individual natural frequency was undertaken to accurately measure the corresponding mode shapes. For these tests, data were acquired at 500 samples per second over a period of 80 seconds.

Modal properties of the bridge model were extracted from the measured sensor data using the stochastic subspace identification (SSI) modal analysis method, as implemented in the commercially available software SPICE (or MACEC) (Van den Branden et al. 1999; Van Overschee and De Moor 1996). For the purposes of modal parameter estimation, it was assumed that the exciting force was not known or measured, so that “output-only” modal extraction techniques were required.

### 2.3 Description of damage cases

Once the baseline dynamic properties of the model had been established, 17 damage states were introduced into the bridge model, including damage to the steel girders, the diaphragm members, the lateral steel straps, the concrete deck, and combinations of these. However, only the three damage cases described in the following paragraph are discussed in this paper.

In Damage Case 1, the bottom plate was removed from the splice at midspan of Girder 4 (SP-X4.0Y2.7 in Fig. 2; see also the inset in Fig. 1), thereby producing a reduction in the flexural rigidity of approximately 32% at that location. Damage Case 2 featured the removal of bolts connecting the bottom ends of the cross-braced diaphragm members at location D-X5.2Y2.25 (see Fig. 2). Similarly, the diaphragm members were disconnected at location D-X8.0Y1.35 for Damage Case 3.

### 2.4 Test protocols investigated

In total, 21 different test protocols were investigated, which included combinations of three different instrumentation schemes (use of accelerometer data, use of data from only the bottom strain gauge in each cluster, and use of data from only the middle strain gauge in each cluster), two different forced excitation methods (resonant harmonic and white noise random), and five different modes. The lowest five vibration modes were extracted when using random excitation, while only the lowest two modes were investigated when using harmonic excitation.



The resulting detailed mode shape definitions and comparisons are available elsewhere (Wang et al. 2008). Other procedures, including the sampling rate, test period, modal extraction method, etc., remained constant for all test protocols.

### 2.5 Description of the VBDD method employed

A new Level 1 VBDD damage indicator (i.e., one capable of identifying the presence, but not location, of damage) was developed for this study, based on the widely used change in mode shape VBDD parameter. Its calculation requires that mode shapes first be scaled using a unit-area normalization procedure. This was achieved by first fitting a natural cubic spline interpolation function to the modal amplitudes at sensor locations along each girder, creating a piecewise cubic polynomial that passed through all the measured amplitudes. The spline function featured continuous first and second derivatives at measurement points, and zero curvature at supports. The individual mode shapes for the four girders were then strung end to end to create a single mode shape vector for the entire structure, and the resulting length of the structure was adjusted to be equal to one. Finally, modal amplitudes were scaled to ensure that the total area under the absolute value of the resulting mode shape function was equal to one. The unit-area normalization scheme was adopted, in part, so that the normalization process would be less sensitive to the number and location of sensors used.

After mode shapes were normalized, the change in mode shape,  $\Delta\phi_{mn}$ , was calculated by

$$\Delta\phi_{mn} = \phi_n - \phi_m, \quad (1)$$

in which  $\phi$  represents a unit-area normalized mode shape vector, including all four girder lines, and the subscripts  $n$  and  $m$  indicate two independently obtained mode shapes. A scalar damage indicator was derived from the change in mode shape vector by calculating the area under  $\Delta\phi_{mn}$ :

$$\Delta A = \int_0^1 |\Delta\phi_{mn}| dx \quad (2)$$

where  $x$  corresponds to the distance along girders (all four included). While the area under the two mode shape vectors,  $\phi_n$  and  $\phi_m$ , are identical by virtue of the unit-area normalization procedure, the distribution of the area over the length of the structure will differ, producing a non-zero area under the difference function. The area of mode shape change,  $\Delta A$ , can therefore be used as an indicator of the presence of damage.  $\Delta A$  can be expected to increase as damage becomes more severe, leading to an increase in the likelihood of detecting the damage.

### 2.6 Procedure used to obtain the resolution of a specific test procedure

Ideally, two independent measurements of a particular mode shape for a structure in the same condition would result in identical unit-area normalized mode shapes. However, uncertainties inherent in the test procedures lead to variability in the measured mode shapes obtained from separate data sets. Thus, a non-zero area of mode shape change,  $\Delta A$ , will be obtained even when the condition of the structure has not changed. The resolution of a particular test protocol can therefore be defined as a threshold value of  $\Delta A$  below which that test protocol is incapable of identifying damage because the observed changes are not statistically significant.

The resolutions of various test protocols were obtained by observing the statistical levels of  $\Delta A$  produced using pairs of mode shapes measured when there was no change in the condition. For the current study, a total of 170 pairs of independently measured mode shapes, in which each mode shape in the pair was obtained from the structure in an identical condition, were used to obtain the statistical variation of  $\Delta A$ . For each pair of mode shapes,  $\phi_n$  and  $\phi_m$ , the change in



mode shape was first obtained using Eq. 1, and the area of mode shape change,  $\Delta A$ , was then calculated.

At this point, it was assumed that the set of 170 values of  $\Delta A$  formed a sample from a normally distributed population. Based on this assumption, the threshold value for  $\Delta A$  was defined as the 95<sup>th</sup> percentile upper exclusion limit—that is, the value that would be exceeded by only 5% of the population. In other words, the threshold value of  $\Delta A$  corresponds to the limiting value above which a calculated change in area would have a 5% probability of occurring when there is, in fact, no change in the condition of the structure (i.e., the probability of a false positive indicator). Thus, if a change in area above the threshold is observed, the chance that the condition of the structure is unchanged is sufficiently small (5%) so as to conclude that a change in condition (i.e. damage) has indeed occurred. It should be acknowledged that, in fact,  $\Delta A$  is likely to follow a non-normal distribution. However, the assumption of a normal distribution permits the method to be illustrated, notwithstanding the need for future refinements.

### 3 EXPERIMENTAL RESULTS AND DISCUSSION

#### 3.1 Threshold values for different test procedures

Table 1 presents the threshold values for area of mode shape change observed for all 21 test protocols investigated, expressed as a percentage of the total area under the original unit-area normalized mode shapes (i.e. 1.0). A smaller threshold value is indicative of a higher resolution for that protocol and a more reliable estimate of mode shapes, which makes the protocol more sensitive to changes in structural condition.

The results presented in Table 1 show that when white noise excitation was used, the use of the fundamental vibration mode obtained by acceleration measurements was clearly superior to all other protocols. Measurement of the fundamental mode using the bottom strain gauges resulted in the next most reliable results, although the threshold value was four times that obtained using acceleration measurements. The use of acceleration measurements to obtain higher modes also produced better resolutions than those obtained by strain measurements, with bottom strain measurements producing the next best results. These trends are similar to those observed previously when other VBDD methods were used (Wang et al. 2008). However, except perhaps for measurements of modes 3 and 5 using accelerometers, threshold values achieved for higher modes were high enough that the protocols would likely be insensitive to all but the most severe of damage cases.

The use of harmonic excitation to measure the fundamental vibration mode resulted in the lowest threshold values of all protocols considered, with all three instrumentation schemes producing similar results. These protocols can therefore be considered to be the most sensitive to changes in structural condition, and therefore the most likely to identify the presence of damage. Interestingly, the protocols making use of strain gauge measurements typically resulted in lower threshold values than those using accelerometer measurements when harmonic

Table 1. Threshold values of area of mode shape change for different test protocols, expressed as percentage of total area under the original unit-area normalized mode shapes.

Instrumentation	White noise excitation					Harmonic excitation	
	Mode 1	Mode 2	Mode 3	Mode 4	Mode 5	Mode 1	Mode 2
Acceleration	0.92%	16.32%	4.65%	23.89%	5.08%	0.33%	4.67%
Bottom strain	3.71%	54.45%	13.36%	41.42%	17.73%	0.28%	2.14%
Middle strain	5.45%	52.01%	18.32%	44.49%	22.79%	0.42%	2.89%



excitation was used, despite the fact that mode shapes generated from accelerometer data have previously been shown to be more reliable than those produced using the strain gauge data (Wang et al. 2008). This might be explained in part by the fact that multiple independent setups were required for acceleration measurements due to the limited number of accelerometers available, whereas the permanently installed strain gauges required only a single setup.

### 3.2 Damage detection

As described in Section 2.3, three damage states were induced in the bridge model after the undamaged dynamic properties had been established: flexural softening at midspan of a girder (Damage Case 1), and disconnecting diaphragm elements (Damage Cases 2 and 3). For each damage case, the area of mode shape change was calculated for only the first vibration mode using Eqs. 1 and 2, in which the damaged and undamaged unit-area normalized mode shape vectors  $\phi_n$  and  $\phi_m$  represented average mode shapes from five separate tests. The resulting area changes in mode shape were then compared to the threshold values presented in the previous section. It is acknowledged that comparing the  $\Delta A$  parameter obtained from averaged mode shapes to threshold values obtained from individual measurements is not strictly consistent. Such a procedure amounts to decreasing the exclusion limit to a very stringent value significantly less than 5%, since 5% exclusion threshold values obtained from averaged mode shapes would be expected to be significantly smaller than those reported in Table 1.

Tables 2 and 3 present the area of mode shape change values obtained for the three damage cases when random and harmonic excitation were used, respectively. The tables also show the ratio of the value obtained to the corresponding threshold value. When the ratio is larger than one, the threshold value has been exceeded, and one can confidently conclude that damage is present, since the observed changes are statistically very significant. On the other hand, the chance of detecting damage using a specific test protocol would be considered low when the corresponding ratio is less than one.

Overall, accelerometers consistently performed better than strain gauges, particularly when random excitation was used. The presence of all three damage cases could be confidently detected using either random or harmonic excitation when accelerometer data were used. On the other hand, the ability to detect damage using a combination of strain gauge data and white noise excitation was relatively low, except when bottom strains were used to detect Damage Case 1. In terms of the preferred excitation method, the data show that, for all instrumentation schemes, harmonic excitation produced consistently higher ratios of actual to threshold values than random excitation (at least 3.7 times higher, except for Case 3 using acceleration data).

## 4 CONCLUSIONS

Several conclusions may be drawn from this study. First, the area of mode shape change parameter,  $\Delta A$ , has been shown to be capable of successfully identifying the presence of damage, and is therefore useful as a level 1 damage indicator.

Secondly, of the 21 test protocols investigated, those that used forced harmonic excitation in

Table 2. Area of change in the 1<sup>st</sup> mode shape due to damage using white noise random excitation.

Instrumentation	Threshold	Area of mode shape change					
		Case 1	Ratio	Case 2	Ratio	Case 3	Ratio
Acceleration	0.92%	6.60%	7.2	1.45%	1.6	1.45%	1.6
Bottom strain	3.71%	6.59%	1.8	1.56%	0.4	1.70%	0.5
Middle strain	5.45%	5.30%	1.0	1.31%	0.2	2.15%	0.4



Table 3. Area of change in the 1<sup>st</sup> mode shape due to damage using harmonic excitation

Instrumentation	Threshold	Area of mode shape change					
		Case 1	Ratio	Case 2	Ratio	Case 3	Ratio
Acceleration	0.33%	8.82%	26.7	2.01%	6.1	0.69%	2.1
Bottom strain	0.28%	7.99%	28.5	1.02%	3.7	0.67%	2.4
Middle strain	0.42%	7.45%	17.5	1.12%	2.6	0.70%	1.6

combination with the fundamental vibration mode consistently resulted in the lowest threshold values for  $\Delta A$ . This held true regardless of whether acceleration or strain measurements were used to represent mode shapes. These protocols are therefore the most sensitive to changes in the structural condition. Random excitation produced much higher threshold values, with only acceleration measurements for the first mode resulting in a threshold value for area change ( $\Delta A$ ) below 1%.

Thirdly, the three damage cases investigated produced areas of changes in the first mode shape that exceeded threshold values when harmonic excitation was used, regardless of the type of instrumentation used to measure mode shapes. Among the instrumentation schemes investigated, both acceleration measurements and strain measurements near the bottom flanges of the girders were able to identify the presence of damage with a high level of confidence. When random excitation was used, the use of acceleration measurements greatly increased the ability to identify the presence of damage, since the protocols using strain measurements produced  $\Delta A$  values that fell close to, or below, threshold values for damage detection.

It is believed that the VBDD method described in this paper, in combination with the protocols identified as being most sensitive to damage, can be used effectively as the initial component of a comprehensive SHM package for bridges by permitting a relatively quick identification of the presence or absence of damage on the structure. An initial assessment using the proposed procedures could then be followed up with a more extensive investigation to locate and quantify the damage, if required.

## 5 ACKNOWLEDGEMENTS

The financial support for this research by the ISIS Canada Network of Centres of Excellence is gratefully acknowledged.

## 6 REFERENCES

- Shrive, P.L. 2005. *Evaluating GFRP and SHM in the Centre Street Bridge Project*. Ph.D. Thesis, University of Calgary, Calgary, Canada.
- Siddique, A.B., Sparling, B.F., and Wegner, L.D. 2007. Assessment of vibration-based damage detection for an integral abutment bridge. *Canadian Journal of Civil Engineering*, 34(3):438-452.
- Wang, Y., Sparling, B.F. and Wegner, L.D. 2008. Vibration-based damage detection on a multi-girder bridge deck, 2nd CSCE International Structural Specialty Conference, Canadian Society for Civil Engineering, Quebec, Quebec, June 10-13, Paper No. ST-302, (CD Rom).
- Wegner, L.D., Zhou, Z., Alwash, M., Siddique, A.B. and Sparling, B.F. 2004. Vibration-based damage detection on bridge superstructures. *Proceedings of the 2nd International Workshop on Structural Health Monitoring of Innovative Civil Engineering Structures*, pp. 429-439.
- Van den Branden, B., Peeters, B., De Roeck G. 1999. *Introduction to MACEC 2, Modal Analysis on Civil Engineering Constructions*, Dept. Civil Engineering. K. U. Leuven, Belgium.
- Van Overschee, P. and De Moor, B. 1996. *Subspace Identification for Linear Systems: Theory - Implementation - Applications*. Kluwer Academic Publishers, Dordrecht, The Netherlands.